Noble isotopic gas fractionation characteristics of China's first batch commercial shale wells in the early production stage

Baojian Shen

State Key Laboratory of Shale Oil and
Gas Enrichment Mechanisms and Effective Development,
Beijing, 100083, China
and
Wuxi Petroleum Geology Institute,
Research Institute of Petroleum Exploration and Production,
Sinopec, Wuxi, 214126, China
Email: shenbj.syky@sinopec.com

Zhiliang He

State Key Laboratory of Shale Oil and
Gas Enrichment Mechanisms and Effective Development,
Beijing, 100083, China
and
China Petroleum and Chemical Corporation,
Beijing, 100728, China
Email: hezhiliang@sinopec.com

Cheng Tao

State Key Laboratory of Shale Oil and
Gas Enrichment Mechanisms and Effective Development,
Beijing, 100083, China
and
Wuxi Petroleum Geology Institute,
Research Institute of Petroleum Exploration and Production,
Sinopec, Wuxi, 214126, China
Email: tc60@sinopec.com

Jincai Shen

SINOPEC Chongqing Fuling Shale Gas Exploration and
Development Co., Ltd.,
Chongqing, 408014, China
Email: shenjinc.jhyt@sinopec.com

Zongquan Hu

State Key Laboratory of Shale Oil and
Gas Enrichment Mechanisms and Effective Development,
Beijing, 100083, China
and
SINOPEC Petroleum Exploration and Production Research Institute,
Beijing, 100083, China
Email: huzongquan.syky@sinopec.com

Zhiming Li

State Key Laboratory of Shale Oil and
Gas Enrichment Mechanisms and Effective Development,
Beijing, 100083, China
and
Wuxi Petroleum Geology Institute,
Research Institute of Petroleum Exploration and Production,
Sinopec, Wuxi, 214126, China
Email: lizm.syky@sinopec.com

Wei Chen*

School of Energy,
Soochow University,
Suzhou, 215006, China
Email: timtamu@suda.edu.cn
*Corresponding author

Abstract: In this study, He and Ar isotope fractionation characteristics in production gases of six Jiaoye shale wells were analysed to identify the fugitive gases occurring in overlying rocks. It was found that both radiogenic ^{40}Ar and ^{4}He concentrations decreased first and then increased due to the release of blocked ^{40}Ar and ^{4}He in the small pores as formation pressure dropped. However, the $^{4}He/^{40}Ar$ ratio slightly decreased since ^{4}He mitigated fast in the shale matrix. In addition, the ratio of radiogenic ^{40}Ar to primordial ^{36}Ar exhibited a monotonic increasing trend due to the degassing of ^{40}Ar from rocks. It is reasonable to assume that there was not convention through the pathway in overlying rocks created by hydraulic fracturing as the concentration difference of $^{3}He/^{4}He$ and $^{40}Ar/^{36}Ar$ between formation and atmosphere did not decrease. Based on noble gases information, the hydraulic fracturing did not destroy the integrity of shale formation overlying rocks. [Received: May 13, 2021; Accepted: January 27, 2022]

Biographical notes: Baojian Shen is a senior specialist of Exploration and Production Research Institute, SINOPEC. He is a Research Fellow, responsible for source rock evaluation and Shale oil and gas geological evaluation. He is an author of more than 40 academic and technical papers.

Zhiliang He is a senior specialist in the SINOPEC. He is mainly engaged in oil and gas geology research, including basin analysis, oil and gas and geothermal geology research.

Cheng Tao is the Chief Engineer in the SINOPEC, Wuxi, China. He is responsible for study of isotopic fractionation, experimental design and the data processing. He is an author of more than 20 technical papers.

Jincai Shen is a senior specialist of Jianghan Oil Field Branch, SINOPEC. He is a Research Fellow, responsible for geological and geochemical evaluation of shale gas. He is the author of more than ten academic and technical papers.

Zongquan Hu is a Research Professor in Petroleum Geology at the Petroleum Exploration and Production Research Institute, SINOPEC. His primary research interest is on shale reservoirs and unconventional petroleum exploration. He is an author of more than 70 academic and technical papers.

Zhiming Li is a senior specialist of Exploration and Production Research Institute, SINOPEC. He is a Research Fellow, responsible for geological and geochemical evaluation of shale oil and gas. He is an author of more than 150 academic and technical papers.

Wei Chen is a Professor at Soochow University. His research interests include nonlinear diffusion and mass transfer mechanisms of gas molecules in porous media and thermal recovery technology of unconventional natural gas resources.

1 Introduction

The successful applications of hydraulic fracturing and horizontal drilling technologies are able to unlock a significant amount of natural gas buried in the shales with ultra-low permeability in China, USA, and elsewhere (Kerr, 2010). Sinopec has achieved a strategic breakthrough for the shale gas exploration in Fuling, Chongqing, China, which is the first commercially and successfully developed shale gas area. It has proven to be the most productive reservoir outside the USA (Nie et al., 2020). However, public environmental concerns including drinking-water contamination and fugitive emissions of hydrocarbons into the atmosphere, are rising due to the fracking industry (Kargbo et al., 2010; Yang et al., 2015). Fugitive gas contamination in a subset of wells near the drill sites are reported by some studies (Osborn et al., 2011; Chen et al., 2020; Hildenbrand et al., 2020). Fugitive hydrocarbon gas migrates from the target shale formations along faults or fractures created, reopened, or intersected by drilling or hydraulic fracturing activities to groundwater and atmosphere (Darrah et al., 2014). Effective well sealing could prevent the leakage of methane and other gases into the groundwater or atmosphere (Davies et al., 2014).

Recently, carbon and hydrogen isotopic gases have been used to examine the water contamination in the active gas-extraction areas (Osborn et al., 2011; Révész et al., 2012). Different from hydrocarbon gases, noble gases are chemically inert and not affected by chemical processes such as chemical reactions or microbial activities (Cao et al., 2018). They are a potentially promising geochemical tracer of migration (Cao et al., 2018). The geochemical properties of helium minimise the interactions with environment as it moves toward the Earth's surface (Barry et al., 2013; Daskalopoulou et al., 2018). Noble gases have been successfully used to understand the gas sources and mitigation pathway contributing to the formation of gas (Byrne et al., 2020). The elemental and isotopic compositions of noble gases can be used to trace the physical processes of shale gas generation and evolution. Among the noble gases, He and Ar isotopes are the two most widespread occurrence in the subsurface and have been used to trace the degassing history of the Earth's mantle, and the migration pathway of hydrocarbons, and to analyse fluid-rock interactions (Holland et al., 2013; Lowenstern et al., 2014). ^{4}He is continuously accumulated in mineral grains of the shale and pore fluids due to α-decay of the ^{235,238}U and ^{232}Th decay chains, and is therefore directly proportional to the concentration of these radio-elements in the crust (Bauer et al., 2016). However, ^{3}He, primordial in origin, is produced by mantle degassing which is the most important terrestrial source (Dong et al., 2019). Helium is highly mobile, and highly diffusive in porous rocks with a diffusion coefficient about ten times that of CO_2 (Daskalopoulou et al., 2018). The isotopic composition of helium – ^{3}He/^{4}He could be used to identify the source of helium and predict the permeability and fracture of rocks (Padrón et al., 2013; Sano and Fischer, 2013). Different from helium, argon has three stable isotopes: ^{36}Ar, ^{38}Ar, and ^{40}Ar, where ^{36}Ar and ^{38}Ar are primordial isotopes whereas ^{40}Ar is generated from the decay of ^{40}K. A small proportion of ^{40}K inside K-bearing minerals decays to ^{40}Ar (Clauer et al., 2020), which makes the sedimentary lithosphere conceivably the source of the most abundant atmospheric argon (Lerman et al., 2007). The ^{40}Ar/^{36}Ar ratios are from 1,650 to 170,000 for the crust, 1,000 to 64,000 for upper mantle, and 295.5 to 8,000 for lower mantle, respectively (Cao et al., 2018; Bekaert et al., 2019; Parai and Mukhopadhyay, 2020).

After being produced by the decay of radioactive elements in the sediment minerals or underlying crustal rocks (Kipfer et al., 2002), ^{4}He and ^{40}Ar diffused into fluid systems like pore water due to its small yield (Barry et al., 2016). Noble gases (e.g., ^{4}He and ^{36}Ar) could be partly soluble in ground water during chemical or biological processes (Padrón et al., 2013), the information of noble gases and their isotopic counterparts such as concentration, composition, and fractionation in natural gases provides complementary evidence on gas source and physical processes that have occurred (Chen et al., 2019). Noble gas isotopes coupled with stable carbon and hydrogen isotopes have been employed to investigate gas mixing, migration and system integrity in conventional natural gas reservoirs (Cao et al., 2018). Darrah et al. (2014) used noble gas and their isotopes to trace the fugitive gas contamination in drinking-water wells and found methane gas migration upward from the gas formation through overlying geological strata triggered by horizontal drilling or hydraulic fracturing. In addition, the concentration anomalies of helium and argon isotopic gases were due to the changes in fracture network connectivity, and the linkages between fluid mitigation and rock deformation (Roques et al., 2020). However, the mechanism of the noble isotopic gas flow characteristics in the produced shale gas, especially the fractionation features, has not been well studied. The lack of understanding of the noble gas variation in the

production gas has prohibited a comprehensive investigation on the shale formation intergrity.

Shale reservoirs in Jiaoshiba areas, Chongqing, have proven to be the best productive wells in China. The environmental risks also spark public concerns regarding the leakage of hydrocarbon to the groundwater or the atmosphere. In this study, the integrity of shale overlying rocks was investigated using Ar and He isotopic gases information. At first, molecular and isotopic composition concentration including radiogram ^{4}He and ^{40}Ar in the production gas of six production wells during the first 50 production months was studied. In addition, the evolution of the ratios of ^{3}He/^{4}He, ^{38}Ar/^{36}Ar, and ^{40}Ar/^{36}Ar was studied to inspect possible faults and fractures for fugitive gas. Finally, the mechanical integrity of the whole shale formation was discussed.

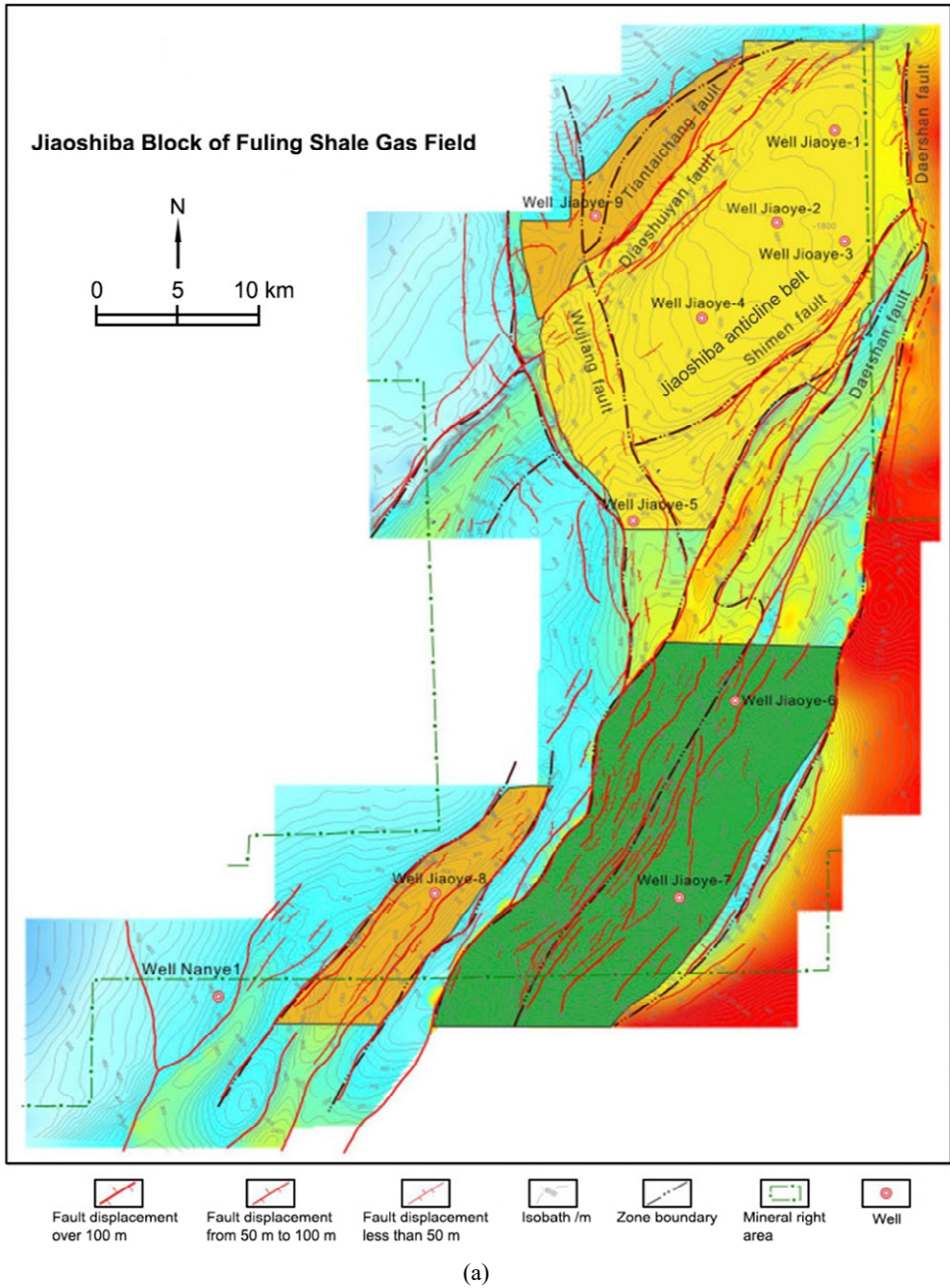## 2 Geological background and methodology

2.1 Geological structure of Fuling shale

In this study, gas samples were collected from six shale wells, including Jiao-1, Jiao-2, Jiao-3, Jiao-4, Jiao-5 and Jiao-6, at Jiaoshiba, Chongqing, China [Figure 1(a)]. The marine shale gas production area developed by Sinopec is located in the Fuling block, Chongqing, China. It is structurally located in the Wanxian complex syncline zone, in the east Sichuan high-steep fold belt in the Sichuan Basin. The Jiaoshiba structure is controlled by two groups of faults trending in east-north direction and nearly north-south direction, separated by fault uplift, broken concave and Qiyueshan Fault [Figure 1(b)] (Guo and Zhang, 2014). The scope of the Fuling block is from 107°05′00″–108°13′00″ east longitude and from 29°16′00″–30°41′00″ north latitude, and the survey area is around 7,307.77 km². The main part of the north is the Jiaoshiba box structure, which belongs to the first-phase development zone.

2.2 Stratigraphic column of Fuling shale

The widespread Upper Ordovician Wufeng-Lower Silurian Longmaxi Formation (Wufeng-Longmaxi Formation) plays an important role in shale gas development (Wang et al., 2020). For example, Jiao-1 shales in the Wufeng-Longmaxi Formation (Figure 2) are characterised by abundant organic matter and high gas contents because of the low sedimentation rate and low-energy anoxic Yangtze shelf environment during the late Ordovician–early Silurian (Qiu and Zou, 2019; Chen et al., 2021). The shale formation shows the vertical variation in lithological composition because of the change in sedimentary environment under different paleoceanographic, paleoclimatic, and paleontological conditions (Yan et al., 2015; Liu et al., 2017; Lu et al., 2020). The upper part of the Longmaxi Formation was characterised by light grey mudstones, and a set of dark grey to black carbonaceous shale mainly deposited at the lower Longmaxi and the Wufeng Formation. It shows a gradual transition from deep water shelf to shallow shelf deposition for long 1 to long 3 in the Fuling area.

Figure 1   (a) The regional geological structure at Fuling shale gas field* (b) Shale gas reservoir
profile in the Fuling area modified from He et al. (2017) (see online version for colours)

(a)

Figure 1 (a) The regional geological structure at Fuling shale gas field* (b) Shale gas reservoir profile in the Fuling area modified from He et al. (2017) (continued) (see online version for colours)
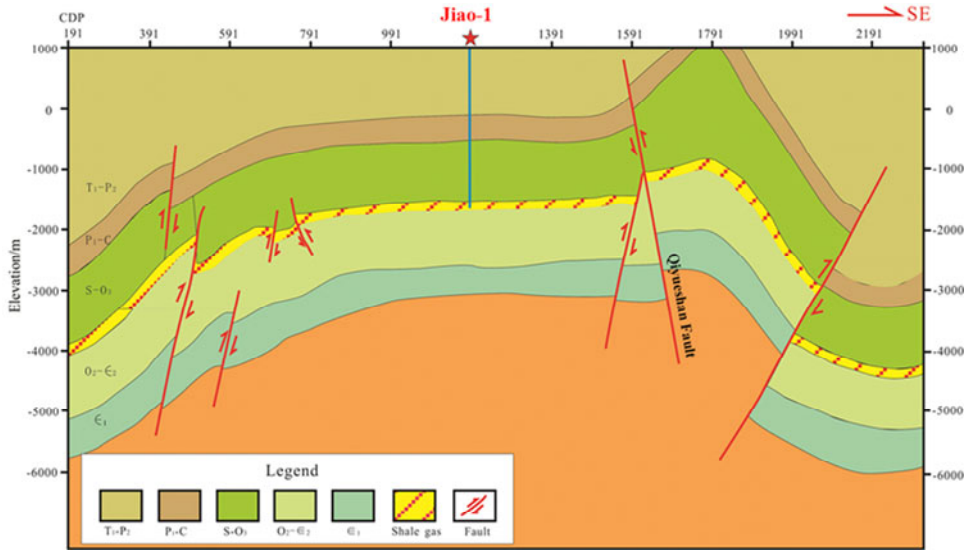
(b)

Source: *modified from Wang (2018)

2.3 Methodology

In order to measure the carbon isotopic gas, fresh gas samples were directly collected from producing well heads using an aluminium alloy (6061) cylinder with a capacity of 700 cm^3. The cylinder was first flushed with the produced gas for 3–5 minutes to avoid air contamination before being sealed with stainless steel clamps. About 700 cm^3 gas was collected in each sealed cylinder for hydrocarbon and noble gas geochemistry analysis. Afterwards, these gas samples were sent to State Key Laboratory of Shale Oil and Gas Enrichment Mechanisms and Effective Development (Sinopec), Wuxi, China for bulk gas composition (mainly CH_4) analysis using gas chromatograph VARIAN 3800. The noble gas compositions (mainly helium and argon) and their stable isotopic compositions (^3He, ^4He, ^{36}Ar, ^{38}Ar, and ^{40}Ar) were measured using noble gas mass spectrometry Noblesse (Nu instruments) according to the commercial code Q/WX0017-2016.

3 Results and discussion

3.1 The integrity of shale formation and noble gas fractionation

Identifying the leakage of hydrocarbon gas through the overlying strata of shale formation can help improve the environmental and economic sustainability of shale-gas industry (Darrah et al., 2014). Thus, the integrity of overlying rock is one of the chief concerns in the successful development of gas extraction industry. In the beginning of production, hydraulic fluid was pumped into shale formation to increase its internal

pressure to fracture the rock. Hydraulic fracturing of shale formation with excessive pressure could also result in the damage of overlying rocks, which creates the faults and fractures as potential preferential pathways for fugitive gases (Figure 3). As a result, it is essential to maintain the hydraulic pressure at a reasonable level to maintain the integrity of the overlying rock. However, it is still challenging to examine the integrity of overlying rock/strata due to the technical detection limitation, especially the small faults or fracture pathways for gas mitigation. The ruptured fractures and faults in the overlying rock may control the amount of He and Ar isotopes in the released fluids (Roques et al., 2020). The abundance of Ar and He isotopes in the production gas could serve as tracers for fluid migration and fluid provenance in crustal system (Darrah et al., 2014). Thus, it provides useful information to examine the overlying rock integrity.

Figure 2   Stratigraphic column of Well Jiao-1 in the Fuling area (see online version for colours)
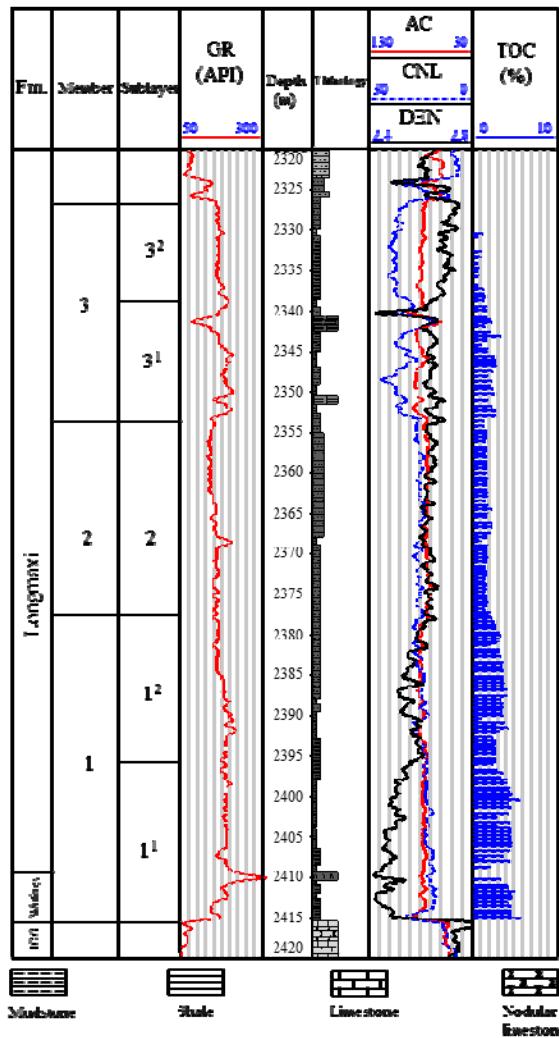
Notes: TOC – total organic carbon; GR – gamma ray; AC – acoustic travel time;
        CNL – compensated neutron; DEN – density log; JCG – Jiancaogou.

Figure 3 The schematic of gas mitigation from shale formation to atmosphere through fractures and faults (see online version for colours)
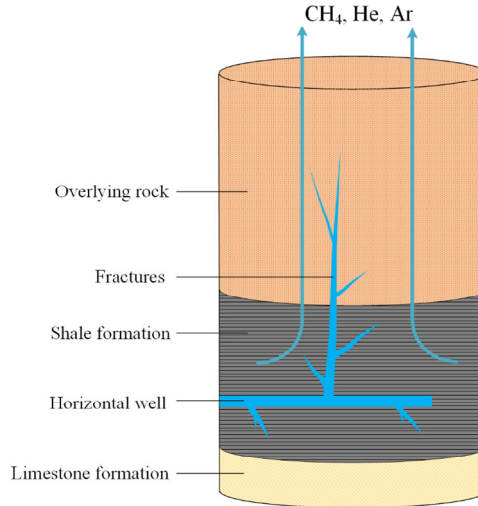
3.2 Gas production rate and formation pressure

During the gas extraction process, gases including the Ar and He noble gases transport from the low permeability porous rocks to the wellhead in well-sealed shale formations. Figure 4 gives the production rate and formation pressure of the six shale wells for the early production period, respectively. It could be found that shale wells had very high production rate during the early stage, especially in the first 30 months. This phenomenon was more obvious for Jiao-1, Jiao-3 and Jiao-6 wells. In the early production stage, the gas production rate was in the range of 150×10^4 m^3/month to 300×10^4 m^3/month. In addition, the shale pressure in the beginning varied from 18 MPa to 30 MPa depending on the wells. Under high formation pressure, the methane gas in the top of the formation could serve as an upper protection layer to prevent gas leakage. With more gas extracted from the reservoir, formation pressure gradually decreased and it reached 5 MPa after 50 months of production. Since isotopic ^{40}Ar and ^{4}He concentrations in shale production gas could provide information of the degree of shale gas source supplied from mineral matrix to fracture network (Cao et al., 2018), these noble gas concentrations were also measured.

3.3 Noble isotopic gas

3.3.1 Abundance of ^{4}He

Since helium isotopes are highly mobile, their isotopic gas releasing signal is sensitive to the rock integrity, which can provide information on the permeability changes and the stress and states in shale (Bauer et al., 2016). In low-permeability shale rocks, it was found that radiogenic ^{4}He mitigates along narrow conduits within geologically-short timescales and results in high concentrations (Byrne et al., 2020). ^{4}He stored in the rock could be transported within the newly created fracture systems. Thus, Faults and fractures of the overlying rocks caused by hydraulic fracking are preferential routes for helium

leakage (Padrón et al., 2012). Based on the test data, ^{4}He abundances in the produced gases ranged from 270 ppm to 430 ppm during the production time (Figure 5). In addition, the concentration of 4He first decreased, and then slightly increased after 30 months of production.

Figure 4   The gas production rate and reservoir pressure of six Jiaoye shale wells in the first-50-month production, (a) Jiao-1 (b) Jiao-2 (c) Jiao-3 (d) Jiao-4 (e) Jiao-5 (f) Jiao-6 (see online version for colours)

(a)

(b)

(c)

(d)

(e)

(f)
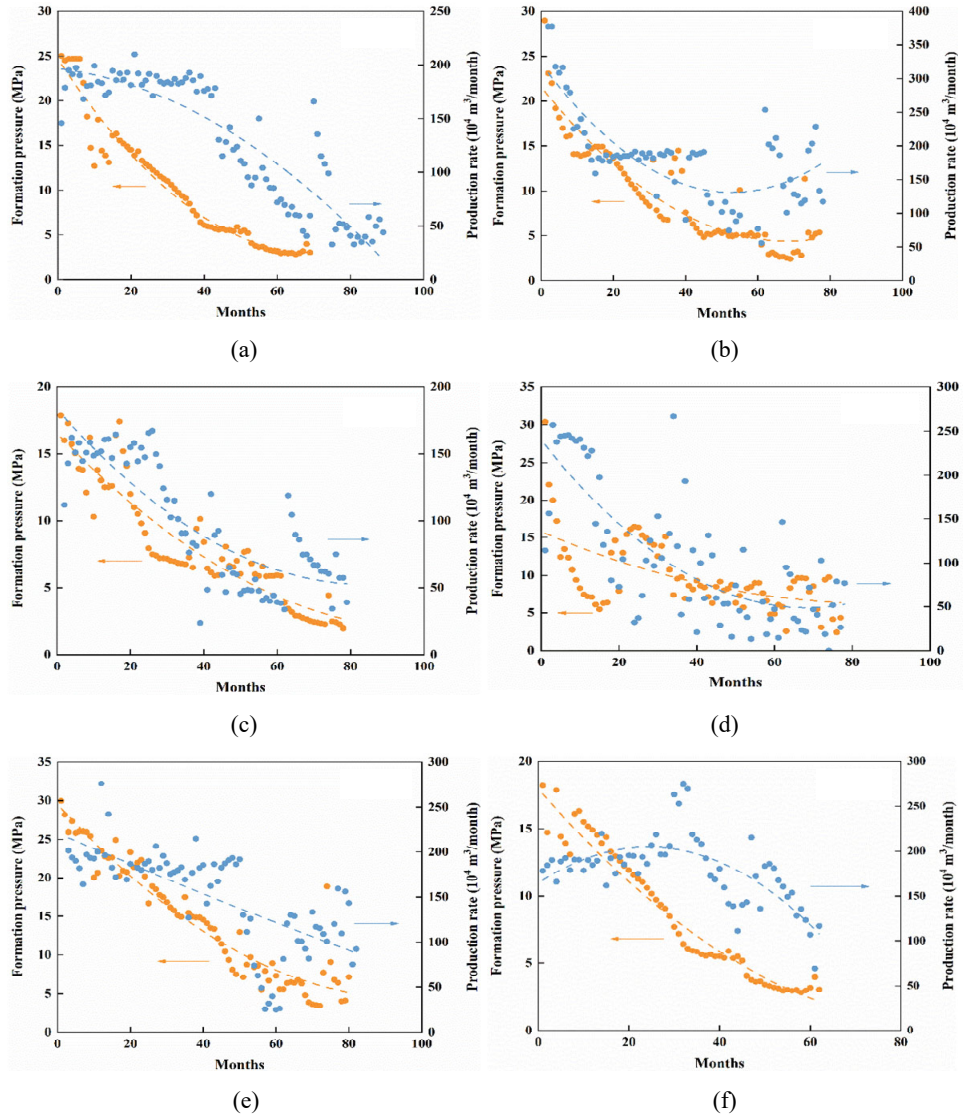
Figure 5 ^{4}He concentration vs. shale gas production time (see online version for colours)
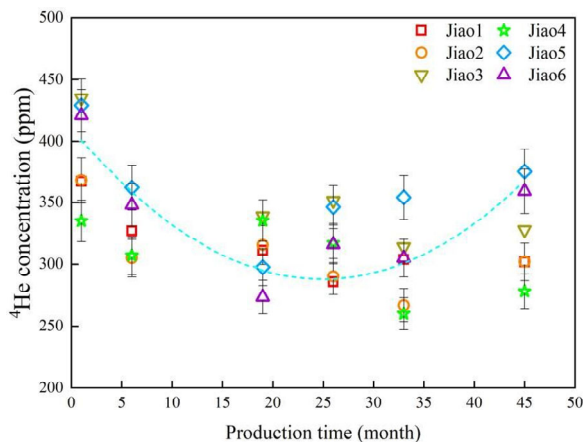
As discussed before, ^{4}He is continuously accumulated in mineral grains and adjacent pore fluids. The helium flux transported from rock grain to the pore fluid in the rock is a function of mineralogy, pore system, fracture network, and formation pressure (Bauer et al., 2016). The major fraction of ^{4}He gas, resulting from radioactive decay of both U and Th, was stored in the macrospores and large fractures at free state or combined with methane gases. Under high formation pressure, the ^{4}He gases were blocked by water molecules in small-size pores such as micropores and mesopores. In addition, helium is almost non-absorbable to the organic matters of shale during the mitigation process (Day et al., 2015). Thus, the total ^{4}He concentration was given as

$$^4\text{He}_{\text{total}} =^4 \text{He}_{\text{free}} +^4 \text{He}_{\text{block}} \tag{1}$$

In the early stage of production, methane gases combined with ^{4}He$_{\text{free}}$ molecules were transported in large fractures and pores to the wellhead. Since ^{4}He$_{\text{free}}$ and ^{4}He$_{\text{block}}$ molecules with less physical mass have much higher 'diffusivity' than methane gases, they mitigated quickly in the shale formation to the wellbore (Cao et al., 2018). This means that produced gases were enriched with free ^{4}He gas in the beginning, and then diluted by high-pressure shale gas during gas degassing in rock matrixes. Thus, ^{4}He concentration in produced gas was relatively rich in the beginning and gradually decreased during the first 25-month production periods. As pressure gradient in the shale formation (after 25 months of production) increased, water molecules could overcome the energy barriers to pass the narrow pore throats of the micropores and mesopores. The original blocked ^{4}He in the nano-sized pores was able to travel to the wellhead and increased the concentration of ^{4}He. Thus, 4Hetotal concentration increased again after 25 months.

According to Figure 4, the formation production pressure all decreased for the six shale wells. For gas flows in the overlying rocks, we consider advection under Darcy's law (Wu et al., 2017).

$$q = -\frac{k_\infty}{\mu} \nabla p \tag{2}$$

where k is the permeability of rock, μ is the shear viscosity of the fluid, and ∇p is pressure gradient between the shale formation and ground. As production went on, ∇p in equation (2) decreased significantly since reservoir pressure decreased. Thus, the chance of helium leakage to the ground through faults and fracture in the overlying rocks created by hydraulic fracking decreased correspondingly. Since the ^{4}He concentration increased after 25 months of production, it was reasonable to assume that the shale formation was still well sealed during the first 50 months of production.

Figure 6   The ^{3}He/^{4}He ratio vs. shale gas production time (see online version for colours)
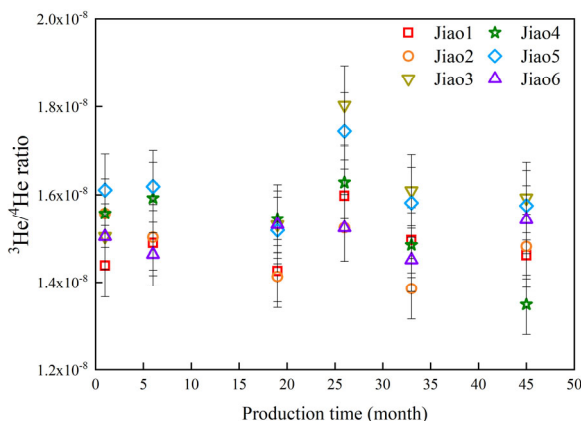
3.3.2   The ^{3}He/^{4}He ratio

Helium isotope ratios such as ^{3}He/^{4}He ratio are often used as indicators of the origin of helium in groundwater or petroleum systems (Wen et al., 2015). In addition, the nature and evolution of ^{3}He and ^{4}He could potentially be used to identify flow paths. Fractures and vertical permeability structures have been found to result in the increase of diffusive helium emission rate (Padrón et al., 2013; Rizzo et al., 2018). Due to rapid diffusivities of He in shale formation, He isotopic gas fractionation is insignificant on the grain scale (Sathaye et al., 2016). The ^{3}He/^{4}He ratios in produced gas varied from 1.35×10^{-8} to 1.8×10^{-8} (Figure 6), or ranged from 0.0096 Ra to 0.0128 Ra (where Ra is the atmospheric value of 1.38×10^{-6}). These values were close to crustal value and the gases were considered to be of crustal origin. These values were much lower than those of atmosphere and sub-continental lithosphere mantle (6.1 Ra) (Jean-Baptiste et al., 2016).

Even through there was a significant difference between the ^{3}He/^{4}He ratios in shale formation and atmosphere, the ^{3}He/^{4}He ratio in the produced gas was in a small range which indicates the convention or diffusion through the pathway in overlying rocks created by hydraulic fracturing was insignificant.

3.4   Argon isotope

3.4.1   The abundance of ^{40}Ar

The abundance of ^{40}Ar in mineral particles is relatively small and it varies from 300 to 600 Ma. The abundance of ^{40}Ar in old illite and K-feldspar is in the order of

10^{-9} mol Ar/g and 10^{-8} mol Ar/g, respectively (Lerman et al., 2007). According to Lerman et al. (2007) ^{40}Ar concentrations in sedimentary clay particles are not in a surface adsorption state. Because of diffusion, radiogenic ^{40}Ar originally accumulated in grains of minerals escapes to the shale pores system and mixes with natural gas (Lerman et al., 2007). Similar to ^{4}He, the ^{40}Ar in the produced gas also includes the free state ^{40}Ar$_{free}$ in large pores and fractures and the original block ^{40}Ar$_{block}$ in small pores such as micropores and mesopores. As a result, the total concentration of ^{40}Ar is given as

$$^{40}\text{Ar}_{total} = {}^{40}\text{Ar}_{free} + {}^{40}\text{Ar}_{block} \tag{3}$$

Figure 7 The ^{40}Ar concentration vs. shale gas production time (see online version for colours)
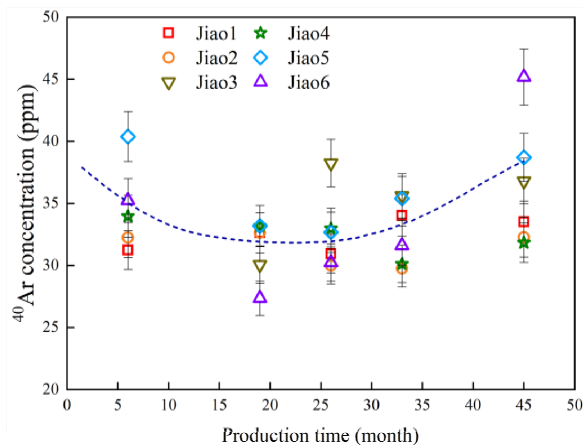
During the production process, the abundance of ^{40}Ar ranged from 26 ppm to 46 ppm (Figure 7). The ^{40}Ar$_{total}$ concentration [equation (3)] decreased slightly and then increased as production went on. Compared to helium, Ar molecules with higher physical mass are less mobile. Diffusivities of He and Ar molecules in minerals differ by orders of magnitude; the diffusion capacity of He out of minerals is geologically much higher than that of Ar at moderate temperatures (Meibom et al., 2003; Ren and Vasconcelos, 2020). Compared to ^{4}He$_{free}$ gas, the concentration of ^{40}Ar$_{free}$ was relatively small and it was diluted by the shale gas in the early production stages. With the decreasing of formation pressure, ^{40}Ar$_{block}$ was able to come out of the small-size pores and enriched in the production gas after 25 months of gas extraction. As a result, ^{40}Ar$_{total}$ gradually increased in the later production stage (from 25 to 50 months).

3.4.2 The ^{4}He/^{40}Ar ratio

From Figure 8, it could be found that ^{4}He/^{40}Ar ratio slightly decreased with production time, ranging from 8 to 12. In addition, the slight decrease of ^{4}He/^{40}Ar ratio in fluids may result from the rapid releasing of noble gases (for example, by fracturing) that have accumulated in porous media which prefers ^{4}He release (Jean-Baptiste et al., 2016). In addition, the high diffusion capacity of ^{4}He molecules relative to heavier ^{40}Ar molecules also resulted in low ^{4}He/^{40}Ar ratio in the produced gas. Thus, the ^{4}He/^{40}Ar ratio decreased as production went on.

Figure 8   The ^{4}He/^{40}Ar ratio vs. shale gas production time (see online version for colours)
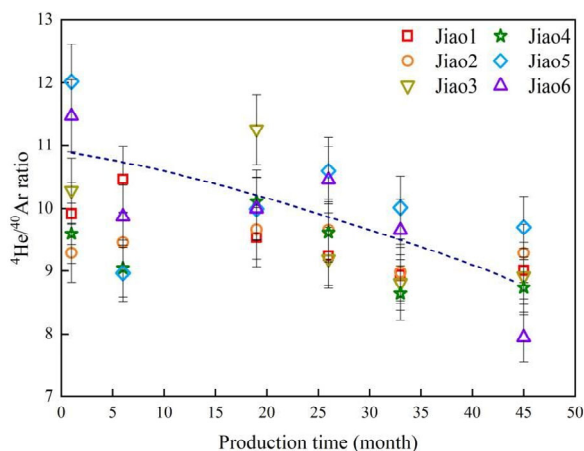
Figure 9   The ^{38}Ar/^{36}Ar ratio vs. shale gas production time (see online version for colours)
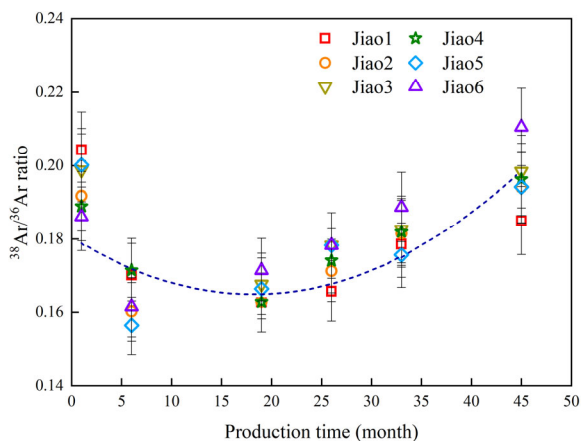
3.4.3   The ^{38}Ar/^{36}Ar ratio

During the production process, mass dependent fractionation of argon isotopic gases occurred. Lighter primordial argon isotopes (^{36}Ar) diffuse preferentially over the heavier isotopes (^{38}Ar). The ^{38}Ar/^{36}Ar ratio in the beginning of the production ranged from 0.1860 to 0.210 (Figure 9), close to the value in air (0.1880) (Raquin and Moreira, 2009). With the production continuing, the ^{38}Ar/^{36}Ar ratio decreased first (below 0.1880), and then gradually increased for all the six shale wells. Compared to ^{38}Ar, ^{36}Ar with less physical mass are more easily desorbed from pore surface and become free state gases. Thus, the produced gas was more enriched with ^{36}Ar and the ^{38}Ar/^{36}Ar ratio decreased in the beginning. With more ^{36}Ar desorbed from the pore surfaces and formation pressure decreased further, ^{38}Ar molecules were triggered to desorb from the pore surface. The produced gas was more enriched with 38Ar with high ^{38}Ar/^{36}Ar ratio.

Figure 10   The $^{40}Ar/^{36}Ar$ ratio of Jiaoye shale gas vs. shale gas production time
(see online version for colours)
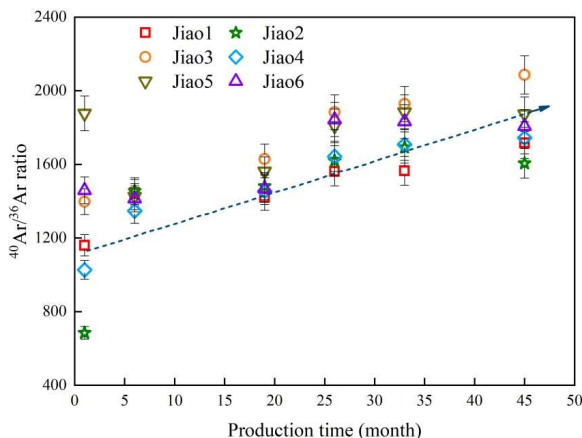
3.4.4   The $^{40}Ar/^{36}Ar$ ratio

Radiogenic argon to primordial argon provide insights into the age accumulative effect from K radiogenic decay and ratios ($^{40}Ar/^{36}Ar$) could be used to monitor the fluid mitigation in response to in situ overlying rock integrity (Cao et al., 2018). The crustal components of shale gases were mostly obtained from Longmaxi marine shale, which was characterised by high $^{40}Ar/^{36}Ar$ contents in the sedimentary rocks (Cao et al., 2018). It was reported that the shale horizontal wells, which are located at the bottom of the Longmaxi Formation, contain U, Th and K elements (Chen et al., 2015). It was found that the $^{40}Ar/^{36}Ar$ ratio exhibited an increasing trend with production time (Figure 10). Argon isotope ratios ($^{40}Ar/^{36}Ar$) of the six shale wells increased from 750 to 1,900, which all exceeded the expected atmospheric equilibrium ratio (295.5 ± 0.5) (Nier and Alfred, 1950; Mark et al., 2011). The difference in $^{40}Ar/^{36}Ar$ ratio in the beginning of production time was caused by regional heterogeneity in Jiaoye regions. As production was going on, radiogenic ^{40}Ar was degassed from rocks after hydraulic fracturing, which increased abundance of ^{40}Ar gas in the production gases. This means the difference of $^{40}Ar/^{36}Ar$ ratio between the atmosphere and shale formation continually increased. As formation pressure dropped, ^{40}Ar molecules were degassed from the minerals and diffused to pore system as supplements. Since ^{36}Ar diffused faster than ^{40}Ar in the shale matrix, mass dependent fractionation of the isotopic gases occurred. The $^{40}Ar/^{36}Ar$ ratio slightly increased in the produced gases. Thus, the concentration difference of ^{40}Ar and ^{36}Ar between shale formation and atmosphere gradually increased. As a result, no equilibrium ratio of [$^{40}Ar/^{36}Ar$] between shale formation and atmosphere also became more intensive, which indicated that the ^{40}Ar and ^{36}Ar leakage in the faults and fractures of overlying rocks created by hydraulic fracking was insignificant (Marty, 2012). Thus, the integrity of the overlying rocks was not destroyed, and the formation rocks were still well sealed so hydrocarbons remained trapped in the reservoir.

4   Conclusions

In this study, He and Ar isotopes in the produced gas fractionation characteristics of six Longmaxi shales during the early production time (first 50 months) were investigated. Based on the fractionation information of He and Ar isotopic gas in the produced shale gas, the integrity of the overlying rock of the shale formation was discussed and the following conclusions were reached.

1 The initial pressure of shale formations varied from 18 MPa to 30 MPa. The gas production rates of the six shale wells were high in the first 30 months and then gradually decreased. The formation pressure gradually decreased to 5 MPa after 50 months of production. During the gas production process, trace amount of He and Ar isotopic gases was detected.

2 During the gas production process, the total concentration of ^{4}He and ^{40}Ar both decreased first and then increased, due to the releasing of original blocked ^{4}He and ^{40}Ar from small-size nanopores as formation pressure decreased. Compared to ^{4}He, the concentration of ^{40}Ar in the six shale wells was in a narrow range from 26 ppm to 46 ppm because of the low mobility of ^{40}Ar.

3 The ^{3}He/^{4}He ratio was in the range of 1.4×10^{-8} to 1.8×10^{-8} (ranging from 0.0096 Ra to 0.0128 Ra), indicating the crustal origin of He isotopic gases. Moreover, the ^{38}Ar/^{36}Ar ratio decreased first, and then increased in the first 50 months, which was mainly ascribed to the mass dependent fractionation during diffusion and adsorption/desorption in the small-size pore system. Moreover, high ^{40}Ar and ^{36}Ar content was found in the sedimentary rocks of Longmaxi Formation. The ratio of radiogenic ^{40}Ar to primordial ^{36}Ar (^{40}Ar/^{36}Ar) exhibited a monotonic increasing trend since heavier ^{40}Ar are richer in the later production period. It varied significantly from 750 to 1,800, exceeding the expected atmospheric equilibrium ratio (295.5 ± 0.5). However, the ^{4}He/^{40}Ar ratio slightly decreased with production time because ^{4}He with less physical mass has high diffusivity rate.

4 The difference of ^{3}He/^{4}He and ^{40}Ar/^{36}Ar ratios between shale formation and atmosphere also did not decrease during the first 50 production months, which meant gas leakage in the faults and fractures of overlying rocks created by hydraulic fracking was insignificant and the integrity of the shale formation overlying rock was not destroyed by hydraulic fracturing.

Acknowledgements

References

Barry, P.H., Hilton, D.R., Fischer, T.P., de Moor, J.M., Mangasini, F. and Ramirez, C. (2013) 'Helium and carbon isotope systematics of cold 'mazuku' CO_2 vents and hydrothermal gases and fluids from Rungwe Volcanic Province, Southern Tanzania', *Chemical Geology*, Vol. 339, pp.141–156.

Barry, P.H., Lawson, M., Meurer, W.P., Warr, O., Mabry, J.C., Byrne, D.J. and Ballentine, C.J. (2016) 'Noble gases solubility models of hydrocarbon charge mechanism in the Sleipner Vest gas field', *Geochimica et Cosmochimica Acta*, Vol. 194, pp.291–309.

Bauer, S.J., Gardner, W.P. and Heath, J.E. (2016) 'Helium release during shale deformation: experimental validation', *Geochemistry, Geophysics, Geosystems*, Vol. 17, No. 7, pp.2612–2622.

Bekaert, D.V., Broadley, M.W., Caracausi, A. and Marty, B. (2019) 'Novel insights into the degassing history of Earth's mantle from high precision noble gas analysis of magmatic gas', *Earth and Planetary Science Letters*, Vol. 525, p.115766.

Byrne, D.J., Barry, P.H., Lawson, M. and Ballentine, C.J. (2020) 'The use of noble gas isotopes to constrain subsurface fluid flow and hydrocarbon migration in the East Texas Basin', *Geochimica et Cosmochimica Acta*, Vol. 268, pp.186–208.

Cao, C., Zhang, M., Tang, Q., Yang, Y., Lv, Z., Zhang, T., Chen, C., Yang, H. and Li, L. (2018) 'Noble gas isotopic variations and geological implication of Longmaxi shale gas in Sichuan Basin, China', *Marine and Petroleum Geology*, Vol. 89, pp.38–46.

Chen, B., Stuart, F.M., Xu, S., Györe, D. and Liu, C. (2019) 'Evolution of coal-bed methane in Southeast Qinshui Basin, China: insights from stable and noble gas isotopes', *Chemical Geology*, Vol. 529, p.119298.

Chen, L., Lu, Y., Jiang, S., Li, J., Guo, T. and Luo, C. (2015) 'Heterogeneity of the Lower Silurian Longmaxi marine shale in the southeast Sichuan Basin of China', *Marine and Petroleum Geology*, Vol. 65, pp.232–246.

Chen, S., Li, X., Chen, S., Wang, Y., Gong, Z. and Zhang, Y. (2021) 'A new application of atomic force microscopy in the characterization of pore structure and pore contribution in shale gas reservoirs', *Journal of Natural Gas Science and Engineering*, Vol. 88, p.103802.

Chen, Y., Li, J., Lu, H. and Xia, J. (2020) 'Tradeoffs in water and carbon footprints of shale gas, natural gas, and coal in China', *Fuel*, Vol. 263, p.116778.

Clauer, N., Środoń, J., Aubert, A., Uysal, I.T. and Toulkeridis, T. (2020) 'K-Ar and Rb-Sr dating of nanometer-sized Smectite-rich mixed layers from Bentonite beds of the Campos Basin (Rio de Janeiro State, Brazil)', *Clays and Clay Minerals*, Vol. 68, No. 5, pp.446–464.

Darrah, T.H., Vengosh, A., Jackson, R.B., Warner, N.R. and Poreda, R.J. (2014) 'Noble gases identify the mechanisms of fugitive gas contamination in drinking-water wells overlying the Marcellus and Barnett Shales', *Proceedings of the National Academy of Sciences*, Vol. 111, No. 39, pp.14076–14081.

Daskalopoulou, K., Calabrese, S., Grassa, F., Kyriakopoulos, K., Parello, F., Tassi, F. and D'Alessandro, W. (2018) 'Origin of methane and light hydrocarbons in natural fluid emissions: a key study from Greece', *Chemical Geology*, Vol. 479, pp.286–301.

Davies, R.J., Almond, S., Ward, R.S., Jackson, R.B., Adams, C., Worrall, F., Herringshaw, L.G., Gluyas, J.G. and Whitehead, M.A. (2014) 'Oil and gas wells and their integrity: implications for shale and unconventional resource exploitation', *Marine and Petroleum Geology*, Vol. 56, pp.239–254.

Day, J.M.D., Barry, P.H., Hilton, D.R., Burgess, R., Pearson, D.G. and Taylor, L.A. (2015) 'The helium flux from the continents and ubiquity of low-^{3}He/^{4}He recycled crust and lithosphere', *Geochimica et Cosmochimica Acta*, Vol. 153, pp.116–133.

Dong, M., Wang, Z-x., Dong, H., Ma, L-c. and Zhang, L-y. (2019) 'Characteristics of helium accumulation in the Guanzhong Basin, China', *China Geology*, Vol. 2, No. 2, pp.218–226.

Guo, T. and Zhang, H. (2014) 'Formation and enrichment mode of Jiaoshiba shale gas field, Sichuan Basin', *Petroleum Exploration and Development*, Vol. 41, No. 1, pp.31–40.

He, Z., Hu, Z., Nie, H., Li, S. and Xu, J. (2017) 'Characterization of shale gas enrichment in the Wufeng Formation-Longmaxi Formation in the Sichuan Basin of China and evaluation of its geological construction-transformation evolution sequence', *Journal of Natural Gas Geoscience*, Vol. 2, No. 1, pp.1–10.

Hildenbrand, Z.L., Carlton, D.D., Wicker, A.P., Habib, S., Granados, P.S. and Schug, K.A. (2020) 'Characterizing anecdotal claims of groundwater contamination in shale energy basins', *Science of the Total Environment*, Vol. 713, p.136618.

Holland, G., Lollar, B.S., Li, L., Lacrampe-Couloume, G., Slater, G.F. and Ballentine, C.J. (2013) 'Deep fracture fluids isolated in the crust since the Precambrian era', *Nature*, Vol. 497, No. 7449, pp.357–360.

Jean-Baptiste, P., Allard, P., Fourré, E., Bani, P., Calabrese, S., Aiuppa, A., Gauthier, P.J., Parello, F., Pelletier, B. and Garaebiti, E. (2016) 'Spatial distribution of helium isotopes in volcanic gases and thermal waters along the Vanuatu (New Hebrides) volcanic arc', *Journal of Volcanology and Geothermal Research*, Vol. 322, pp.20–29.

Kargbo, D.M., Wilhelm, R.G. and Campbell, D.J. (2010) 'Natural gas plays in the Marcellus Shale: challenges and potential opportunities', *Environmental Science & Technology*, Vol. 44, No. 15, pp.5679–5684.

Kerr, R.A. (2010) 'Natural gas from shale bursts onto the scene', *Science*, Vol. 328, No. 5986, pp.1624–1626.

Kipfer, R., Aeschbach Hertig, W., Peeters, F. and Stute, M. (2002) 'Noble gases in lakes and ground waters', *Reviews in Mineralogy & Geochemistry*, Vol. 47, pp.615–700.

Lerman, A., Ray, B.M. and Clauer, N. (2007) 'Radioactive production and diffusional loss of radiogenic ^{40}Ar in clays in relation to its flux to the atmosphere', *Chemical Geology*, Vol. 243, No. 3, pp.205–224.

Liu, Z., Algeo, T.J., Guo, X., Fan, J., Du, X. and Lu, Y. (2017) 'Paleo-environmental cyclicity in the Early Silurian Yangtze Sea (South China): tectonic or glacio-eustatic control?', *Palaeogeography, Palaeoclimatology, Palaeoecology*, Vol. 466, pp.59–76.

Lowenstern, J.B., Evans, W.C., Bergfeld, D. and Hunt, A.G. (2014) 'Prodigious degassing of a billion years of accumulated radiogenic helium at Yellowston', *Nature*, Vol. 506, No. 7488, pp.355–358.

Lu, Y., Hao, F., Lu, Y., Yan, D., Xu, S., Shu, Z., Wang, Y. and Wu, L. (2020) 'Lithofacies and depositional mechanisms of the Ordovician-Silurian Wufeng-Longmaxi organic-rich shales in the Upper Yangtze Area, Southern China', *AAPG Bulletin*, Vol. 104, No. 1, pp.97–129.

Mark, D.F., Stuart, F.M. and de Podesta, M. (2011) 'New high-precision measurements of the isotopic composition of atmospheric argon', *Geochimica et Cosmochimica Acta*, Vol. 75, No. 23, pp.7494–7501.

Marty, B. (2012) 'The origins and concentrations of water, carbon, nitrogen and noble gases on Earth', *Earth and Planetary Science Letters*, Vols. 313–314, pp.56–66.

Meibom, A., Anderson, D.L., Sleep, N.H., Frei, R., Chamberlain, C.P., Hren, M.T. and Wooden, J.L. (2003) 'Are high ^{3}He/^{4}He ratios in oceanic basalts an indicator of deep-mantle plume components?', *Earth and Planetary Science Letters*, Vol. 208, No. 3, pp.197–204.

Nie, H., Li, D., Liu, G., Lu, Z., Hu, W., Wang, R. and Zhang, G. (2020) 'An overview of the geology and production of the Fuling shale gas field, Sichuan Basin, China', *Energy Geoscience*, Vol. 1, Nos. 3–4, pp.147–164.

Nier and Alfred, O. (1950) 'A redetermination of the relative abundances of the isotopes of carbon, nitrogen, oxygen, argon, and potassium', *Phys. Rev.*, Vol. 77, No. 6, pp.789–793.

Osborn, S.G., Vengosh, A., Warner, N.R. and Jackson, R.B. (2011) 'Methane contamination of drinking water accompanying gas-well drilling and hydraulic fracturing', *Proc. Natl. Acad. Sci. USA*, Vol. 108, No. 20, pp.8172–8176.

Padrón, E., Pérez, N.M., Hernández, P.A., Sumino, H., Melián, G., Barrancos, J., Nolasco, D. and Padilla, G. (2012) 'Helium emission at Cumbre Vieja Volcano, La Palma, Canary Islands', *Chemical Geology*, Vols. 312–313, pp.138–147.

Padrón, E., Pérez, N.M., Hernández, P.A., Sumino, H., Melián, G.V., Barrancos, J., Nolasco, D., Padilla, G., Dionis, S., Rodríguez, F., Hernández, Í., Calvo, D., Peraza, M.D. and Nagao, K. (2013) 'Diffusive helium emissions as a precursory sign of volcanic unrest', *Geology*, Vol. 41, No. 5, pp.539–542.

Parai, R. and Mukhopadhyay, S. (2020) 'Heavy noble gas signatures of the North Atlantic Popping Rock 2ΠD43: implications for mantle noble gas heterogeneity', *Geochimica et Cosmochimica Acta*, Vol. 294, pp.89–105.

Qiu, Z. and Zou, C. (2019) 'Controlling factors on the formation and distribution of 'sweet-spot areas' of marine gas shales in South China and a preliminary discussion on unconventional petroleum sedimentology', *Journal of Asian Earth Sciences*, Vol. 194, p.103989.

Raquin, A. and Moreira, M. (2009) 'Atmospheric 38Ar/36Ar in the mantle: implications for the nature of the terrestrial parent bodies', *Earth and Planetary Science Letters*, Vol. 287, No. 3, pp.551–558.

Ren, Z. and Vasconcelos, P.M. (2020) 'Mechanisms and kinetics of argon diffusion in hypogene and supergene jarosites: implications for geochronology and surficial geochemistry on Earth and Mars', *Geochimica et Cosmochimica Acta*, Vol. 289, pp.207–224.

Révész, K.M., Breen, K.J., Baldassare, A.J. and Burruss, R.C. (2012) 'Carbon and hydrogen isotopic evidence for the origin of combustible gases in water-supply wells in north-central Pennsylvania', *Applied Geochemistry*, Vol. 27, No. 1, pp.361–375.

Rizzo, A.L., Pelorosso, B., Coltorti, M., Ntaflos, T., Bonadiman, C., Matusiak-Małek, M., Italiano, F. and Bergonzoni, G. (2018) 'Geochemistry of noble gases and CO₂ in fluid inclusions from lithospheric mantle beneath Wilcza Góra (Lower Silesia, Southwest Poland)', *Frontiers in Earth Science*, Vol. 6, p.215.

Roques, C., Weber, U.W., Brixel, B., Krietsch, H., Dutler, N., Brennwald, M.S., Villiger, L., Doetsch, J., Jalali, M., Gischig, V., Amann, F., Valley, B., Klepikova, M. and Kipfer, R. (2020) 'In situ observation of helium and argon release during fluid-pressure-triggered rock deformation', *Scientific Reports*, Vol. 10, No. 1, p.6949.

Sano, Y. and Fischer, T.P. (2013) 'The analysis and interpretation of noble gases in modern hydrothermal systems', in Burnard, P. (Ed.): *The Noble Gases as Geochemical Tracers*, Springer, Berlin, Heidelberg.

Sathaye, K.J., Smye, A.J., Jordan, J.S. and Hesse, M.A. (2016) 'Noble gases preserve history of retentive continental crust in the Bravo Dome Natural CO₂ Field, New Mexico', *Earth and Planetary Science Letters*, Vol. 443, pp.32–40.

Wang, L., Dong, Y., Zhang, Q. and Duan, R. (2020) 'Numerical simulation of pressure evolution and migration of hydraulic fracturing fluids in the shale gas reservoirs of Sichuan Basin, China', *Journal of Hydrology*, Vol. 588, p.125082.

Wang, Z. (2018) 'Reservoir forming conditions and key exploration and development technologies for marine shale gas fields in Fuling area, South China', *Petroleum Research*, Vol. 3, No. 3, pp.197–209.

Wen, T., Castro, M.C., Ellis, B.R., Hall, C.M. and Lohmann, K.C. (2015) 'Assessing compositional variability and migration of natural gas in the Antrim Shale in the Michigan Basin using noble gas geochemistry', *Chemical Geology*, Vol. 417, pp.356–370.

Wu, L., Ho, M.T., Germanou, L., Gu, X-J., Liu, C., Xu, K. and Zhang, Y. (2017) 'On the apparent permeability of porous media in rarefied gas flows', *Journal of Fluid Mechanics*, Vol. 822, pp.398–417.

Yan, D., Wang, H., Fu, Q., Chen, Z., He, J. and Gao, Z. (2015) 'Geochemical characteristics in the Longmaxi Formation (Early Silurian) of South China: implications for organic matter accumulation', *Marine and Petroleum Geology*, Vol. 65, pp.290–301.

Yang, H., Thompson, J.R. and Flower, R.J. (2015) 'Improve oversight of fracking in China', *Nature*, Vol. 522, No. 7554, pp.34–34.